

Electronic Supplementary Information

Photochemical and electrochemical reduction of graphene oxide thin films: tuning the nature of surface defects

Javier A. Quezada Renteria^{a,b}, Cristina Ruiz-García^a, Thierry Sauvage^a, Luis F. Chazaro-Ruiz^b, Jose R. Rangel-Mendez^b, Conchi O. Ania*^a

Table S1. Elemental Analysis (wt.%) of the pristine bulk GO. Data has been recalculated as at.% for comparison purposes.

Table S2. Layer Thickness and atomic concentrations of oxygen, carbon and nitrogen of the studied thin films, as extracted from NRA analyses. Film thicknesses were obtained in at. \cdot cm $^{-2}$; a density value of 1.9 g \cdot cm $^{-3}$ (GO without porosity) was used to convert at. \cdot cm $^{-2}$ units in metric system.

Table S3. Fitting parameters calculated for all samples upon deconvolution of the first and second order Raman spectra.

Figure S1. (left) Thermogravimetric profile of pristine GO compared to graphite powders used as precursor; (right) selected m/z signals of the gases evolved upon the thermal analysis detected by a mass-spectrometer coupled to the thermobalance.

Figure S2. X-ray diffraction patterns of the synthesized GO compared to the graphite used as precursor.

Figure S3. Temperature evolution of the electrolytic solution during the photochemical irradiation of the electrodes.

Figure S4. Cyclic voltammograms recorded at 2 mV/s in a neutral aqueous electrolyte for the series of thin film electrodes supported on ITO glass substrate: (A) cycles on GO electrode, to obtain ErGO; (B) cycles on PhrGO electrode, to obtain EPhrGO.

Figure S5. Deconvolution of the C1s core spectra of A) GO, B) ErGO, C) PhrGO, D) PhErGO and E) EPhrGO.

Figure S6. NRA spectra of samples GO, ErGO and EPhrGO.

Figure S7. Deconvolution of the O1s core spectra spectra of A) GO, B) ErGO, C) PhrGO, D) PhErGO and E) EPhrGO.

Figure S8. Deconvolutions of the Raman spectra (first and second order) of the studied samples.

Table S1. Elemental Analysis (wt.%) of the pristine bulk GO. Data has been recalculated as at.% for comparison purposes.

	Carbon	Sulphur	Hydrogen	Oxygen	Nitrogen
GO (wt.%)	49.51	2.06	1.83	46.60	0
GO (at.%)	46.53	0.72	19.9	32.85	0

Table S2. Layer Thickness and atomic concentrations of oxygen, carbon and nitrogen of the studied thin films, as extracted from NRA analyses. Film thicknesses were obtained in at. \cdot cm $^{-2}$; a density value of 1.9 g \cdot cm $^{-3}$ (GO without porosity) was used to convert at. \cdot cm $^{-2}$ units in metric system.

Sample	layer thickness (x10 ¹⁵ at. \cdot cm $^{-2}$)	layer thickness (nm)	Carbon (at.%)	Oxygen (at.%)	Nitrogen (at.%)
GO	2000 \pm 100	230 \pm 10	62 \pm 2	32 \pm 1	6 \pm 2
ErGO	1650 \pm 100	190 \pm 10	82 \pm 2	18 \pm 1	< 1
PhrGO	1100 \pm 100	130 \pm 10	80 \pm 2	20 \pm 2	< 1
EPhrGO	2500 \pm 100	290 \pm 10	82 \pm 2	18 \pm 1	< 1
PhErGO	800 \pm 100	100 \pm 10	81 \pm 2	19 \pm 2	< 1

Table S3. Fitting parameters calculated for all samples upon deconvolution of the first and second order Raman spectra.

		D*	D	D''	G	D'	X	2D	G+D	2D'
	Peak Type	Gauss	Voigt	Gauss	Voigt	Voigt	Voigt	Lorentz	Lorentz	Lorentz
GO	Area (%)	0.77	44.03	7.56	12.91	8.30	1.40	8.22	15.42	1.41
	Center (cm ⁻¹)	1110	1354	1510	1566	1610	1725	2709	2916	3190
	Max Height	0.018	1.000	0.225	0.618	0.658	0.049	0.131	0.216	0.029
	FWHM (cm ⁻¹)	177	132	141	67	53	119	188	219	150
ErGO	Area (%)	0.35	46.50	4.52	15.06	6.66	0.40	9.98	14.72	1.81
	Center (cm ⁻¹)	1149	1354	1506	1584	1610	1725	2708	2934	3179
	Max Height	0.009	1.000	0.136	0.542	0.466	0.013	0.129	0.190	0.049
	FWHM (cm ⁻¹)	130	109	112	87	48	82	186	189	88
PhrGO	Area (%)	0.78	37.07	4.74	18.03	6.59	0.099	8.46	20.74	3.48
	Center (cm ⁻¹)	1149	1353	1478	1583	1616	1725	2710	2936	3178
	Max Height	0.027	1.000	0.161	0.769	0.643	0.016	0.181	0.309	0.094
	FWHM (cm ⁻¹)	130	117	131	72	40	27	146	218	119
EPhrGO	Area (%)	0.57	44.70	3.51	13.96	7.03	0.59	10.84	16.34	2.45
	Center (cm ⁻¹)	1149	1354	1504	1583	1610	1725	2702	2934	3188
	Max Height	0.015	1.000	0.126	0.523	0.512	0.020	0.146	0.224	0.056
	FWHM (cm ⁻¹)	130	109	97	87	48	82	186	184	110
PhErGO	Area (%)	3.10	44.88	4.82	17.00	6.74	1.43	8.91	11.64	1.48
	Center (cm ⁻¹)	1149	1354	1500	1586	1610	1725	2705	2940	3188
	Max Height	0.052	1.000	0.175	0.643	0.496	0.049	0.105	0.162	0.033
	FWHM (cm ⁻¹)	211	119	97	87	48	82	211	179	110

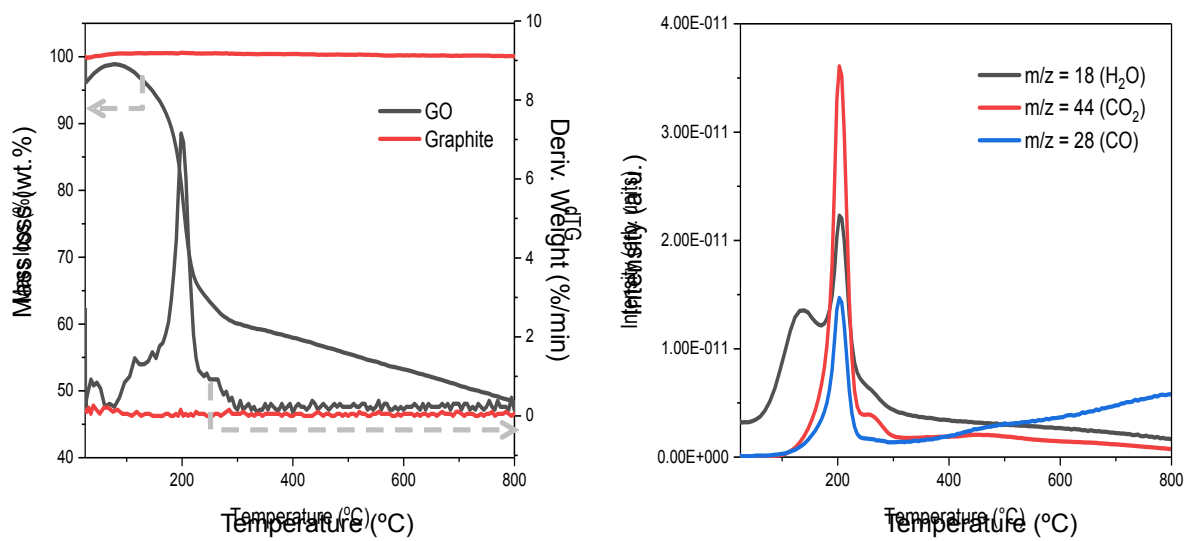


Figure S1. (left) Thermogravimetric profile of pristine GO compared to graphite powders used as precursor; (right) selected m/z signals of the gases evolved upon the thermal analysis detected by a mass-spectrometer coupled to the thermobalance.

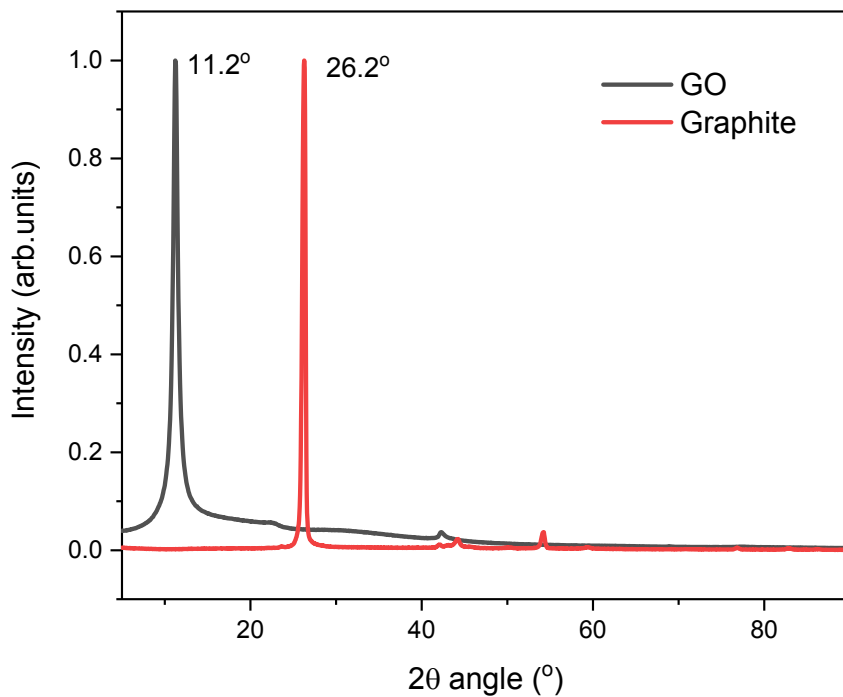


Figure S2. X-ray diffraction patterns of the synthesized GO compared to the graphite used as precursor.

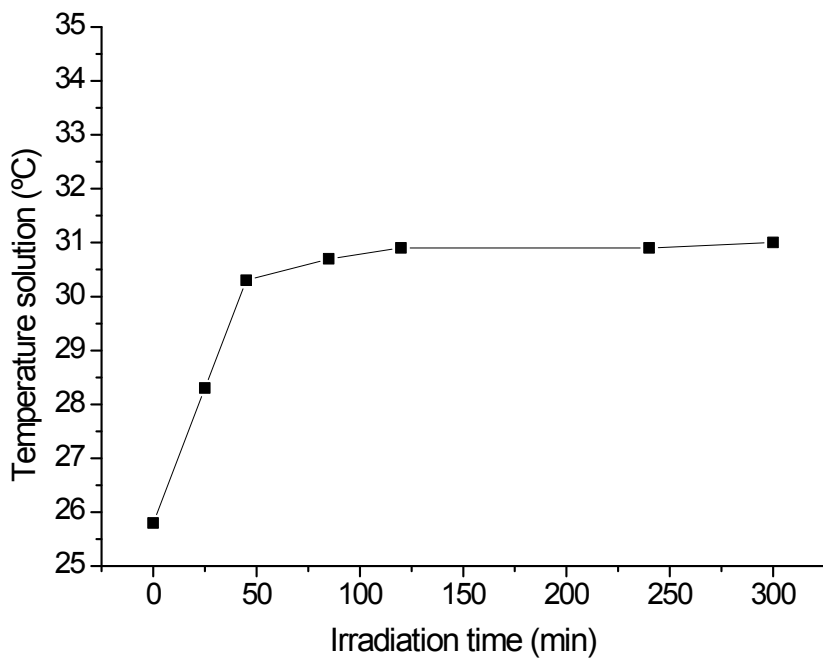


Figure S3. Temperature evolution of the electrolytic solution during the photochemical irradiation of the electrodes

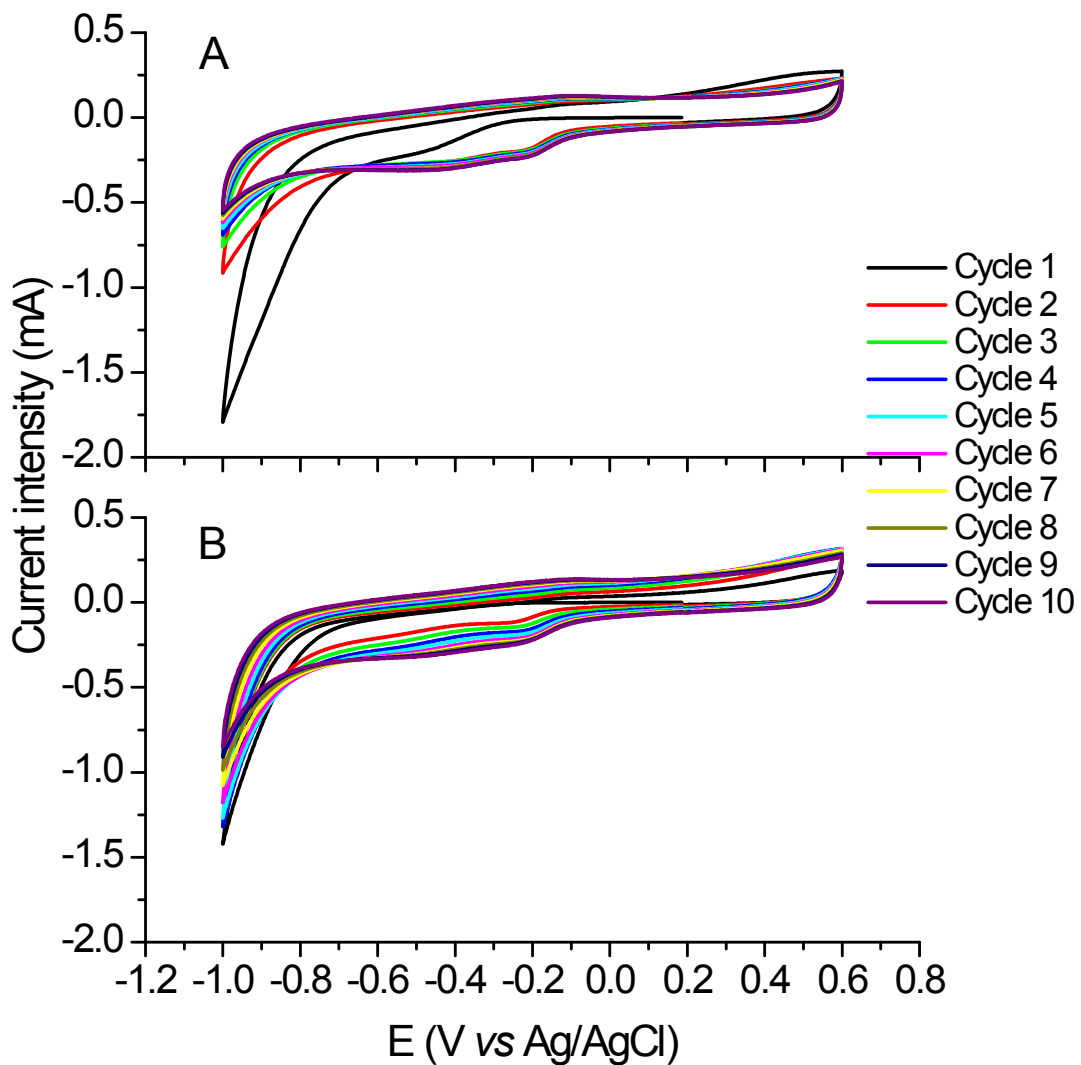


Figure S4. Cyclic voltammograms recorded at 2 mV/s in a neutral aqueous electrolyte for the series of thin film electrodes supported on ITO glass substrate: (A) cycles on PhrGO electrode to obtain PhErGO; (B) cycles on GO electrode, to obtain ErGO.

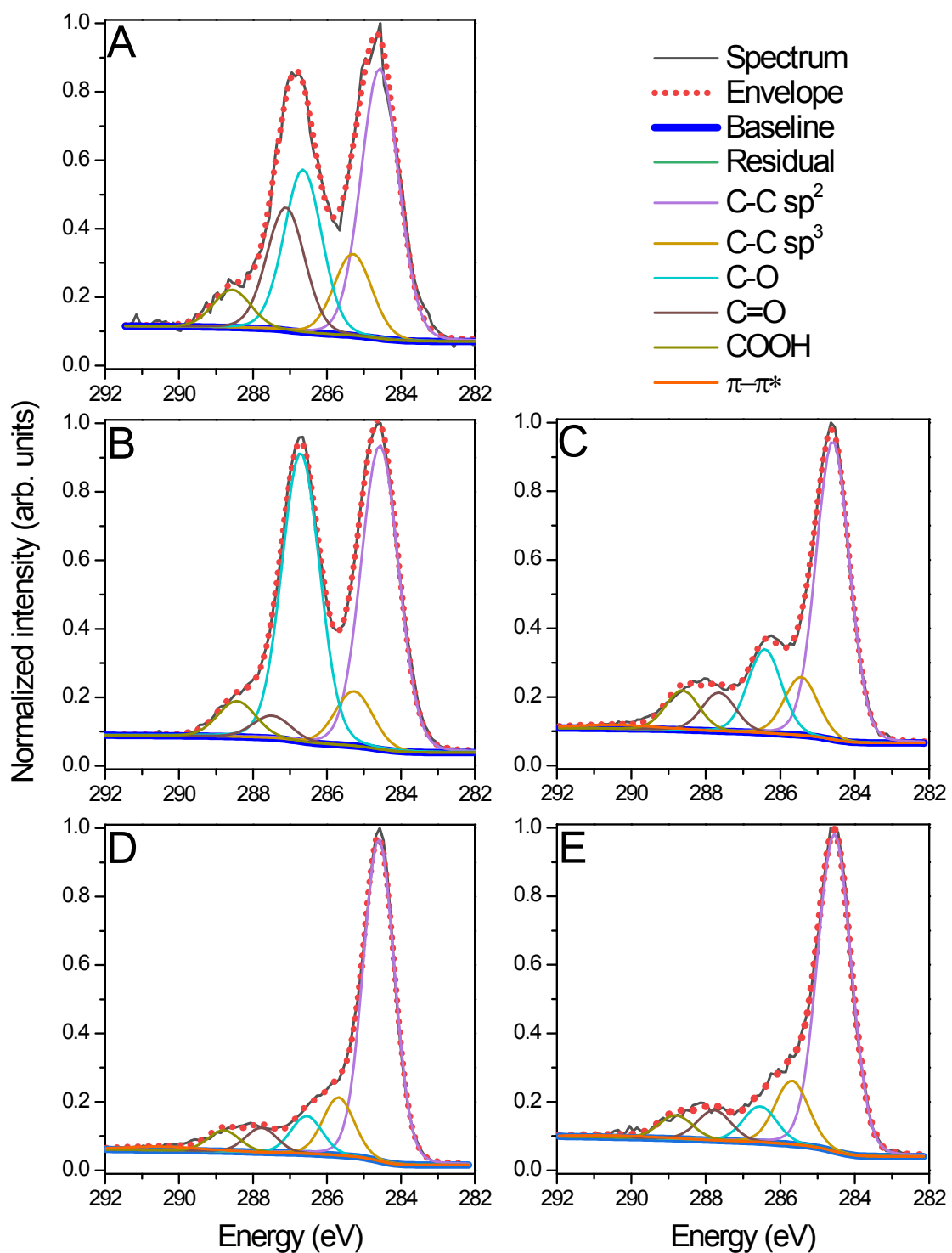


Figure S5. Deconvolution of the C1s core spectra of A) GO, B) ErGO, C) PhrGO, D) PhErGO and E) EPhrGO.

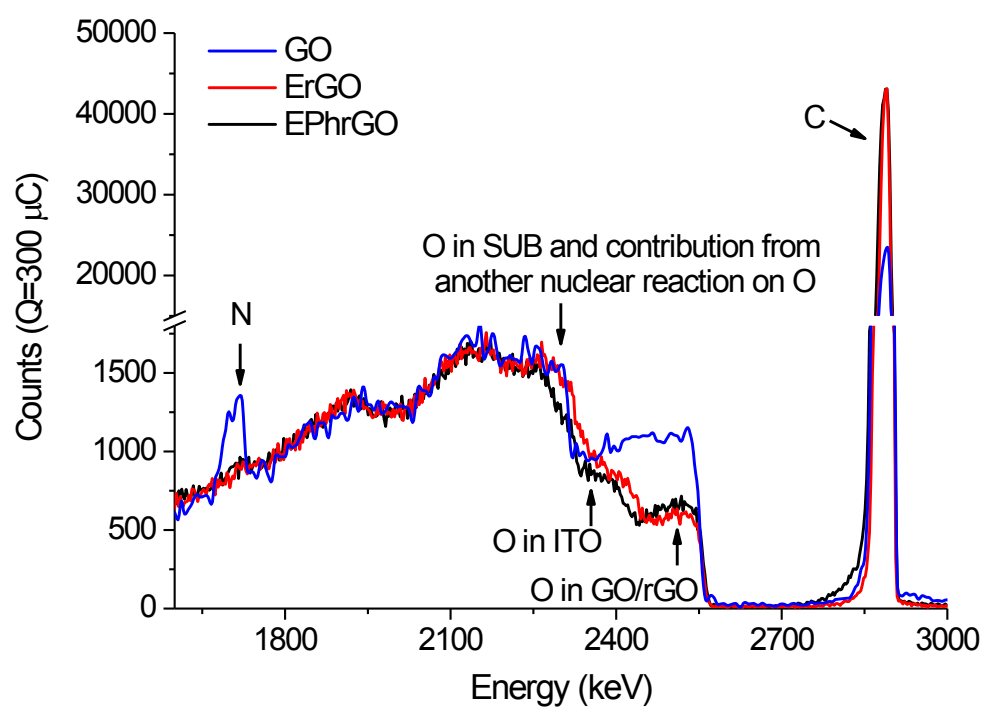


Figure S6. NRA spectra of samples GO, ErGO and EPhrGO.

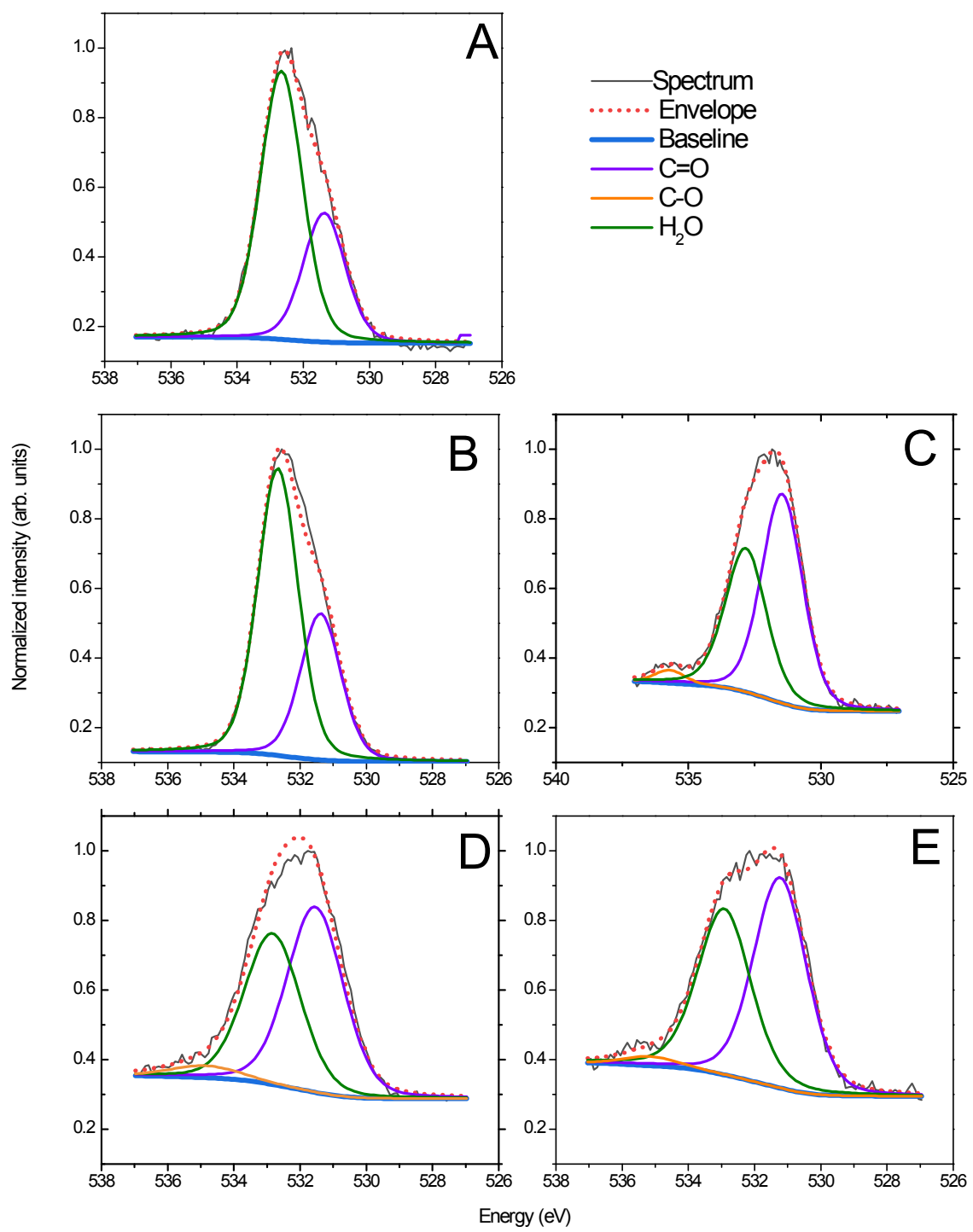


Figure S7. Deconvolution of the O1s core spectra of A) GO, B) ErGO, C) PhrGO, D) PhErGO and E) EPhrGO

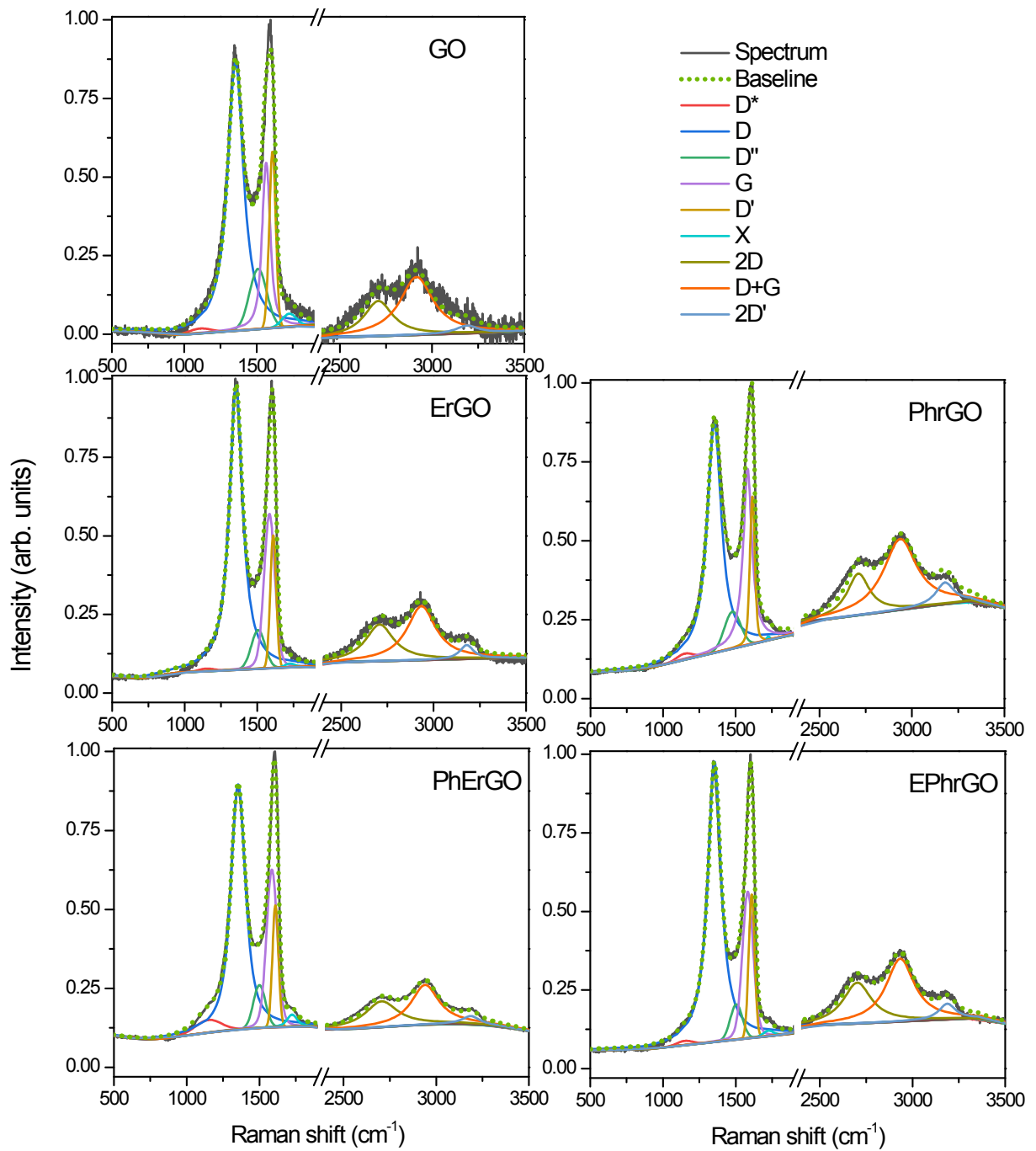


Figure S8. Deconvolutions of the Raman spectra (first and second order) of the studied samples.